

FACILE TPO DISPERSION USING EXTENSIONAL MIXING

Stéphane Costeux, Mark Barger, Keith Luker*, Anand Badami, Kim Walton
The Dow Chemical Company, Midland, MI (U.S.A.)

*Randcastle Extrusion Systems, Inc., Cedar Grove, NJ (U.S.A.)

Abstract

The mixing performance of a small-scale extensional mixer (SFEM) was benchmarked against a mixing bowl. TPO blends of 70% polypropylene and 30% ethylene copolymers were chosen for this evaluation, with a broad range of elastomer melt indices. Various statistical metrics were evaluated to quantify the degree of dispersion of the blends.

The conclusion is that due to stronger extensional flow, the SFEM batch mixer indeed has potential to offer better TPO dispersion than mixers with rotors in which shear dominates. A single-screw extruder equipped with SFEM mixing elements achieved even finer dispersion, usually achievable only with twin screw extruders.

Introduction

Small scale batch mixing or compounding is a common need in R&D for formulation screening of polymeric blends or composites. It is typically used in situations where:

- Very small amounts of one or more of the components are available
- Numerous compositions need to be screened by a test that only requires a small quantity of the composite
- If reactive chemistry is expected to take place during mixing, it is typically more prudent to proceed at a small scale.

The most important attribute of mixing equipment used to make such small scale blends is that it achieves a degree of mixing or morphology that is consistent with that obtained with large scale compounding equipment. If the geometry of the batch mixer is very different from the mixing element geometry of the large-scale process (often involving a single-screw extruder), translation of laboratory formulation results to commercial scale becomes extremely challenging.

Several comparisons of common micro-batch mixers, including batch internal mixers with rotors (later referred to as “Mixing bowl”) [1], miniature conical twin screws with a recirculation [1,2], dual pistons capillary mixers [3,4] or chaotic mixers [5] can be found in the literature. Generally, mixing bowls normally provide homogeneous (distributive) mixing due to the kneading action and friction of its rotor blades on the molten

polymer, and are often a good choice for miscible blends. Other mixers are sometimes more effective for immiscible blends (dispersive mixing) when they use high shear and elongation, but have limitations for highly viscous polymer systems where shear heating becomes significant.

Elongational forces are more effective than shear forces to achieve breakdown and dispersion of polymeric domains, as shown on the classical plot by Grace [6] in Figure 1. The capillary number is expressed of the stress, τ , of the interfacial tension, σ , and average droplet radius, R , as

$$Ca_c = \frac{\tau}{\sigma / R}, \text{ with } \tau = \eta \dot{\gamma} \text{ or } \tau = \eta_E \dot{\epsilon}$$

depending on the type of deformation (shear rate $\dot{\gamma}$ or extension rate $\dot{\epsilon}$, respectively, η being the corresponding matrix viscosity). The break-up threshold is higher for shear than for extension, and is more sensitive to λ , so that higher stress are needed to break-up domains when λ is significantly different from 1. In particular, when the viscosity ratio exceeds about 3.5, the dispersed droplets can deform under simple shear but can no longer break.[6,7] This limitation does not exist for extensional flow. This constitutes a good test for mixers which claim making use of extensional flow as the primary dispersion mechanism.

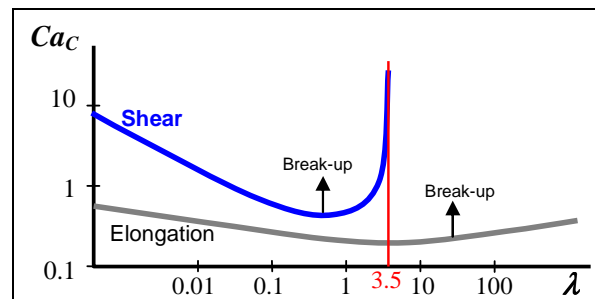


Figure 1. Critical capillary number, Ca_c , above which droplet break-up is possible, vs. viscosity ratio, λ (viscosity of dispersed phase over that of the matrix).

A spiral fluted extensional mixer (later referred to as SFEM), introduced by Randcastle Extrusion Systems in 2008 [8] is shown in Figure 2. The flow entering the mixing element is split into two halves, each composed of three flutes or channels (C1, C2, C3) and two intermediate pumps (P1 and P2). The hypothesized mixing mechanism is that the melt enters channel C1, and due to the rotation, a fraction of the material is dragged

into the thin clearance P1 where it is sheared. Channel C2 allows for shear interruption, as the molten material remains in the vicinity of the barrel wall, and enters C3 by the flight P2. Maximum elongation occurs between P1 and P2 and in the entrance flow of the narrow clearances. Recirculation takes place as the material flows along the channels (spiral flow) which contributes to distributive mixing. Once in channel C3, the melt is conveyed to the second half to repeat the process in the opposite direction. While conceptually similar to a Maddock mixing element, the oblique flutes of the SFEM are able to force material along the channels and maintain lower pressure drops than longitudinal flutes.

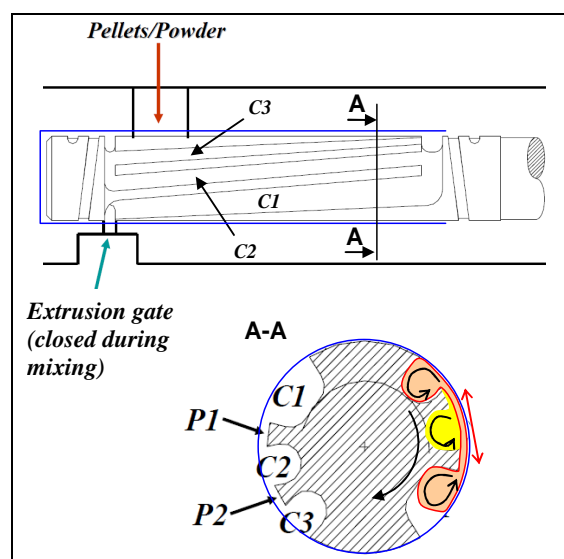


Figure 2. Geometry of the SFEM mixing element, showing the oblique channels C1-C3. Extension is maximal next to the barrel wall between the clearances P1 and P2

Experimental

Melts of polypropylene (PP) and ethylene/ α -olefin copolymers (EAO) are known to exhibit limited compatibility and form blends having low-medium interfacial adhesion, which make them good candidate to test the ability of a mixer to break down polymer domains (dispersive mixing). The dispersion of ethylene-based elastomers into PP has been shown to improve toughness when the average domain size is below 2 to 3 microns, either by promoting a large number of small crazes [9] (above 0.5 microns), or by shear-yielding for smaller elastomer domains, [10] which benefits impact resistance. PP-EAO compatibility and dispersion is known to depend on alpha-olefin type [11] and level [12]. However, the ability to mechanically disperse PE-based domains in this range is a good criterion to assess

TPO mixing performance of the SFEM compared to a mixing bowl.

Materials

INSPIRE HST 404 (D404.01) is a high crystalline polypropylene with a melt flow rate (MFR, 2.16 kg, 230°C) of 3 dg/min. The five ethylene/ α -olefin elastomers (EAO) used in this study are listed in Table 1. Due to their density and comonomer type, EG8130 and HM7280 are expected to have respectively better and worse PP-compatibility than the other three EAO.

Table 1. Characteristics of the EAO elastomers

EAO resin	Comonomer Type	MI* (dg/min)	Density (g/cc)	Viscosity ratio λ (100 1/s) [#]
EG 8407	Octene	30	0.870	0.2
EG 8130	Octene	13	0.864	0.5
EG 8200	Octene	5	0.870	0.8
EG 8150	Octene	0.5	0.868	2.7
HM 7280	Butene	<0.1	0.884	4.8

* MI at 2.16kg, 190°C; [#] viscosity EAO / viscosity D404

Figure 3 shows the shear viscosity of the six polyolefins at 200°C. The viscosity of D404 is similar to that of Engage 8150 and Engage 8200 at low and high (100 1/s) shear rates respectively.

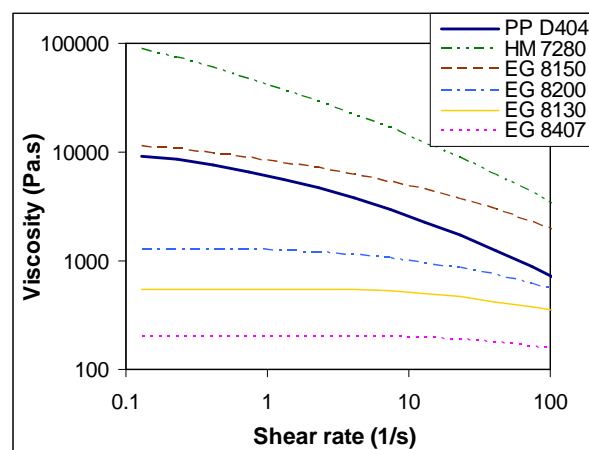


Figure 3. Viscosity of the polyolefin blend components at 200°C (from small angle oscillatory shear)

Compounding

Batch Mixing Bowl samples were prepared using a Haake Rheomix 900 equipped with a 50cc mixing bowl. Temperature was set to 200°C. Polymers (35g PP and 15g EAO) were premixed, and added to the bowl. Mixing at 60 RPM was maintained for 10 min.

Batch SFEM mixing was carried out with a 25 mm diameter rotor ($L/D=4$). Clearances P1 and P2 have a clearance of 1 mm. TPO blend components pellets (7g PP and 3g EAO) were premixed, added to the feed port and pushed in the mixer with a feeding ram (input time = 1 minute), and then processed at 204°C for 3 minutes at a rotor speed of 100 RPM. After mixing, the rotor was stopped and the die gate was opened. The rotor was re-started to induce extrusion of a molten strand of 5 to 6 cc.

Extrusion mixing of PP D404 with EG8150 and EG8130 (70wt% PP, 30wt% EAO) with the SFEM was carried out at Randcastle Extrusion Systems with a single screw extruder equipped with a 1", 36 L/D screw with three SFEM elements [13]. All heating zones were set to 204°C (400F), the screw speed was 100 RPM and the output rate 10 lbs/hr. The extruded blend was pelletized.

Morphology

All the blends were compression-molded into 0.5 mm thick plaques at 200°C, trimmed using an automated CNC Cryo-Mill at -100 °C and cryopolished at -100 °C.

Ambient tapping mode Atomic Force Microscopy (AFM) was performed on samples 1, 2, 3, and 6 using a Digital Instruments Dimension 3100 with a Nanoscope IV controller and a NSC14 silicon probe (Mikromasch) with a radius of curvature <10 nm. Samples 4, 5, and 7 through 12 were imaged using a Veeco Icon with a Nanoscope V controller and a NSC16 silicon probe (Mikromasch) Typical ambient tapping conditions were $A_0 \sim 2000$ mV and A_{sp}/A_0 of 0.85 with a scan rate of 0.8 to 1.0 Hz. Images were acquired at a scan size of $30 \mu\text{m} \times 30 \mu\text{m}$ at 512 or 1024 lines of resolution.

The AFM images were analyzed with the ImageJ (NIH) software using the "Analyze particle" function after binarization. All domains with an area larger than 10 pixels were included in the analysis. The analysis yielded a collection of cross-sectional area, A_i , for all domains in the $30\mu\text{m} \times 30\mu\text{m}$ image. The size of each domain, D_i , was calculated as the diameter of a disk of the same cross-sectional area:

$$D_i = \sqrt{4A_i / \pi}.$$

Histograms were built for the number and volume distributions, from which additional statistical information was obtained.

Discussion

The morphology of blends made with the Mixing Bowl and the batch SFEM are shown in Figure 4. It is immediately apparent that larger domains are present for

all the Mixing Bowl samples compared to the batch SFEM samples, which show distinctive elongation of the domains at low viscosity ratios. The two extruded samples are shown in Figure 5. Comparison with Figure 4 indicates finer dispersion than batch mixed analogs.

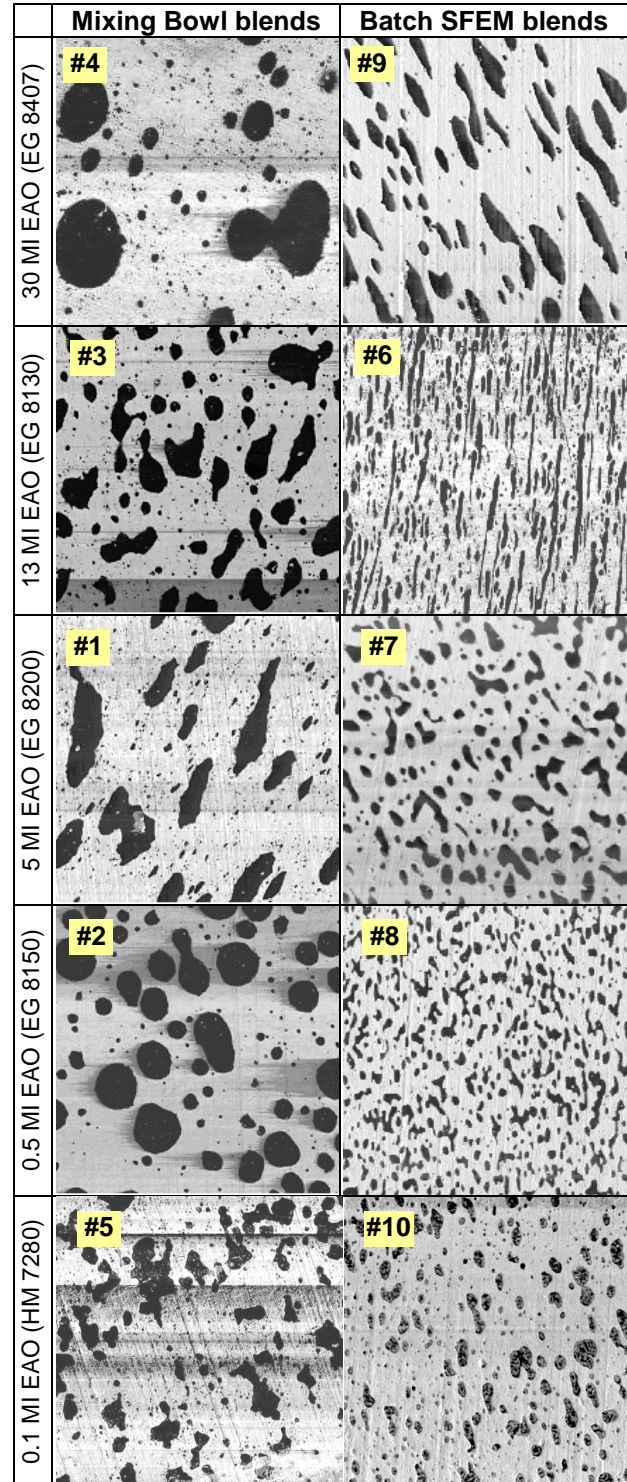


Figure 4. AFM images ($30\mu\text{m} \times 30\mu\text{m}$) of morphology of blends made with 5 EAO using two batch mixers.

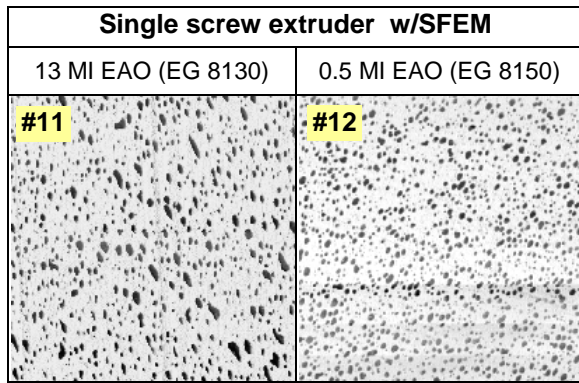


Figure 5. AFM images (30µm x 30µm) of morphology of blends made by extrusion with the SFEM elements

To improve the quantitative assessment of the difference between the three processes, histograms were built for both the number and volume distribution of domain size (i.e. the number fraction $n(D_j)$ and volume fraction $v(D_j)$ that domains of diameter D_j account for). The number distribution is very heavily biased towards small domain sizes, and ignores the presence of a few large, non-dispersed domains. On the other hand, the volume dispersion is biased towards these large domains.

Figure 6 shows the number and volume distributions for the blends made with EG8150 using the three mixing processes. Comparison of $n(D)$ and $v(D)$ for sample #2 shows the fingerprint of highly bimodal distribution, with the number peak around 0.3-0.5 µm, and the volume peak around 3 to 5 µm. This is illustrative of large domains accounting for almost all the volume, in a sea of debris formed by abrasion of the large domains in high shear. On the other extreme, sample #12 shows two narrow peaks for $n(D)$ and $v(D)$ located between 0.3 to 1 µm. Note the similarity of $n(D)$ between the two samples. $V(D)$ is therefore a better differentiator of the degree of dispersion. The third sample, #8, also has overlapping $n(D)$ and $v(D)$, each peak being broader than sample #12, but without the bimodal nature of sample #2.

Statistical information calculated from the distributions for all the blends are compiled in Table 2, and will be used to determine most relevant metrics of the degree of dispersion:

- Number of domains (# domains), maximum domain size seen in each AFM image (Max)
- Means of the number and volume distribution, D_n and D_v . Dispersity index is the ratio of D_v to D_n .
- Number fraction of domains that exceed 1 µm, and Volume fractions of domains larger than 1 or 3µm
- 85th percentile of the two distributions, e.g. $V(85\%)$ is the size such that 85 vol% of the domains are smaller, i.e. the size corresponding to a

value of the cumulative volume distribution equal to 0.85:

$$\int_0^{V(85\%)} v(x)dx = 0.85 \quad \text{with} \quad \int_0^{\infty} v(x)dx = 1$$

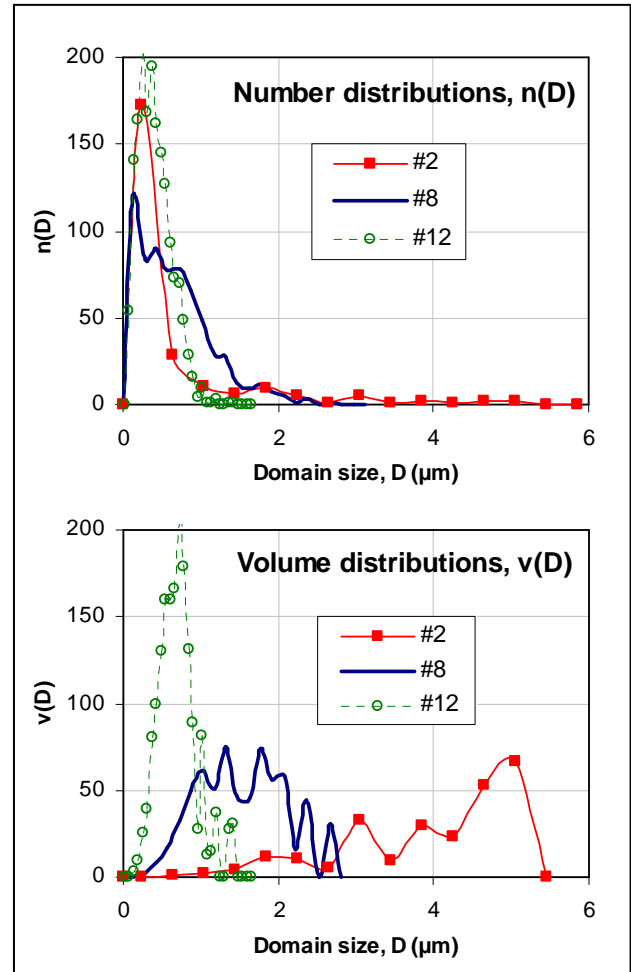


Figure 6. Number and volume domain size distribution of 70% PP + 30% EG8150 made by three compounding methods (#2: Mixing Bowl; #8: batch SFEM; #12: SFEM Extruder)

Large domains are not favorable for mechanical properties of the TPO, and are evidence that the mixing intensity is insufficient. Thus the two desirable features for the domain size distributions are a low fraction of large domains, and a narrow domain size distribution.

The former can be measured by the Volume mean, Max, or the 85th percentile. Max depending on the single largest domain, it is more sensitive than $V(85\%)$ to the choice of the AFM image analyzed.

The latter can be estimated by the dispersity index, or equivalently by the ratio of $V(85\%)$ to $N(85\%)$.

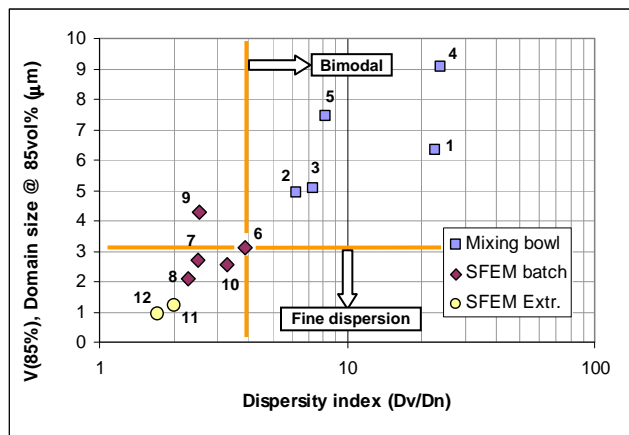


Figure 7. Dispersion map: volume distribution 85th percentile, V(85%) vs. Dispersity index

The map showed in Figure 7 provides a way to classify the degree of dispersion, i.e. the efficiency of the mixing. A low value of V(85%) is a good indicator of a finely dispersed blends, as it indicates the absence of large domains that represent a significant fraction of the total volume. The dispersity index measures the separation between the main peaks in the number and volume distributions, so that a high value is a strong indication of a bimodal blend where large domains coexist with numerous smaller domain, likely resulting from shear abrasion.

In Figure 7, a criterion for fine, monomodal domain size distribution corresponds to the lower left quadrant on the dispersity map. The blends made with the SFEM extruder meet this criterion, together with the blends produced with the SFEM batch with medium to high viscosity ratios. The fact that droplets in the HM 7280 blends which have the highest viscosity ratio (estimated λ is 4.8, larger than the shear break-up limit of 3.5 [6]) and the lower compatibility with PP are dispersed supports the claim that the flow in the SFEM is primarily elongational, based on the Grace plot. Therefore, it is probable that the elongated domains in samples #6 and #9 (Batch SFEM, low viscosity ratio) exceeded the capillary number criterion, yet have not undergone break up due to insufficient mixing time. This issue is not present with the single screw extruder, in which the total mixing time is increased by the use of 3 SFEM elements.

Conclusions

The results of the evaluation of the Randcastle SFEM batch mixer indicate that its dispersive capabilities are superior to the Mixing Bowl, while reducing the amount of material and time per blend. It is confirmed that the SFEM's primary deformation mode is elongational, which also contributes to limiting shear

heating effects. The same SFEM elements can be added to a single screw extruder, which achieve even better performance, which is encouraging from a scale-up standpoint. This technology is suitable for single-screw extrusion of TPOs and other immiscible blends.

References

1. P. Walia, M. Barger, M. McKelvy, "Quantitative Mixing Uniformity Assessment In Two Laboratory Scale Devices", *SPE ANTEC*, 265-270 (2005)
2. M. Marić and C. W. Macosko, "Improving polymer blend dispersion in mini-mixers", *Polym. Eng. & Sci.*, **41**, 118-130 (2001).
3. M. Bouquey, C. Loux, B. Triki and R. Muller, "a new type of mixer based on elongational flow: preliminary results on polymer blends", *Proc. of the ICBC-2008*, Kottayam, Kerala, India
4. D. Kim, Y. Son, "Development of a novel micro-compounder for polymer blends and nano-composites" *SPE ANTEC*, 2142-2146 (2006)
5. A. Dhoble *et al.*, "Mechanical properties of PP-LDPE blends with novel morphologies produced with a continuous chaotic advection blender", *Polymer*, **46**, 2244-2256 (2005)
6. H.P. Grace, "Dispersion phenomena in high viscosity immiscible fluid systems and application of static mixers as dispersion devices in such systems", *Chem Eng. Commun.*, **14**, 225 (1982)
7. L.A. Utracki, "Polymer blends handbook", Vol 1, p16 (2002)
8. K. Luker, "A novel micro-batch mixer that scales to a single screw compounder", *SPE ANTEC*, 1400-1404 (2008)
9. B. Z Jang, D. R. Uhlmann, J. B. Vander Sande, "The Rubber Particle Size Dependence of Crazing in Polypropylene", *Polym Eng Sci*, **25**, 643 (1985).
10. J. Z. Liang and R. K. Y. Li, "Rubber toughening in polypropylene: A review", *J. Appl. Polym. Sci.*, **77**, 409-417 (2000).
11. M. Kontopoulou *et al.*, "Effect of composition and comonomer type on the rheology, morphology and properties of ethylene- α -olefin copolymer/polypropylene blends", *Polymer*, **44**, 7495-7504 (2003)
12. D. Mäder *et al.*, "Influence of Comonomer Incorporation on Morphology and Thermal and Mechanical Properties of Blends Based upon Isothermal Metallocene-Polypropylene and Random Ethene/1-Butene Copolymers", *J. Appl. Polym. Sci.*, **74**, 838-848 (1999).
13. K. Luker, T.M. Cunningham, "Investigation Into A High Output Polypropylene Screw And Its Mixing Mechanism", *SPE ANTEC*, 1197-1204 (2009)

Acknowledgements

We thank Dow colleagues Devin Foether and Dennis Lantz for their help with sample preparation, Kenny Lloyd and Jeff Bonekamp for providing the resins, and Joe Chiaravalle at Randcastle Extrusion Systems for help

producing blends. The Dow Chemical Company is acknowledged for permitting publication.

Key Words: Blends, Polyolefin, TPO, batch mixer, extensional deformation, single-screw extruder

Table 2. Statistics on domain size distributions

	Mixing Bowl					Batch SFEM					SSE w/ SFEM	
	30	13	5	0.5	0.1	30	13	5	0.5	0.1	13	0.5
MI (l_2) EAO (dg/min)	#4	#3	#1	#2	#5	#9	#6	#7	#8	#10	#11	#12
Sample ref												
# domains	411	235	829	192	144	99	702	260	470	456	988	1200
Max (μm)	9.08	5.10	6.32	5.05	7.42	4.38	3.28	2.93	2.66	2.84	1.52	1.41
Number mean (μm)	0.327	0.504	0.217	0.635	0.682	1.256	0.466	0.856	0.670	0.525	0.427	0.408
Volume mean (μm)	7.802	3.685	4.884	3.974	5.560	3.183	1.805	2.132	1.538	1.723	0.853	0.700
Dispersity index	23.89	7.32	22.54	6.26	8.15	2.53	3.87	2.49	2.29	3.28	2.00	1.71
N% > 1 μm	4.62	12.61	2.41	16.67	16.40	46.15	11.92	34.31	21.62	16.01	3.74	1.00
V% > 1 μm	99.35	98.72	98.67	98.88	99.10	98.91	84.68	94.89	81.60	88.22	33.53	11.37
V% > 3 μm	94.17	81.10	87.24	85.82	82.45	53.87	15.54	0.00	0.00	0.00	0.00	0.00
N(85%) (μm)	0.37	0.73	0.24	1.26	1.25	2.56	0.86	1.58	1.12	1.01	0.68	0.64
V(85%) (μm)	9.07	5.07	6.31	4.93	7.42	4.30	3.13	2.70	2.10	2.54	1.22	0.92